

EXPERIMENTAL INVESTIGATION ON NONLINEAR CHARACTERISTICS OF A HIGH-TEMPERATURE SUPERCONDUCTING DUAL-BAND BANDPASS FILTER

Shoichi Narahashi¹, Kei Satoh¹, Yasunori Suzuki¹, and Yuta Takagi¹

¹Research Laboratories, NTT DOCOMO, INC., 3-6 Hikari-no-oka, Yokosuka, Kanagawa, Japan
{narahashi, satokei, suzukiyasu, takagiyu}@nttdocomo.co.jp

Keywords: Dual-band, Bandpass Filter, Superconductor, Intermodulation Distortion, Third-order Intercept Point

Abstract: This paper presents an experimental investigation on the nonlinear characteristics of a high-temperature superconducting (HTS) dual-band bandpass filter (DBPF) that has two passbands and comprises a coplanar-waveguide quarter-wavelength resonator with odd- and even-mode resonant frequencies. An HTS filter is a potential candidate for an RF multi-band bandpass filter (MBPF) that has multiple passbands, which will support broadband transmission in future mobile communication systems. It is, however, indispensable to elucidate the nonlinear characteristics of the HTS-MBPF because the nonlinearity of HTS materials causes intermodulation distortion (IMD). This paper presents the IMD characteristics of a 2.0-/3.5-GHz band HTS-DBPF using a YBCO thin film deposited on a MgO substrate when two tones with a 30-kHz separation are individually and simultaneously input to each passband. Experimental investigations confirm that the HTS-DBPF generates different third-order IMD characteristics depending on how the two tones are input to the HTS-DBPF. This paper also presents a method for estimating the third-order IMD characteristics based on the measurement results.

1 INTRODUCTION

In recent years, Carrier Aggregation (CA) has attracted attention as a technology for improving transmission speeds in future mobile communication systems (Miki, Iwamura, Kishiyama, Anil & Ishii 2010). CA achieves broadband transmission using several fundamental frequency blocks (referred to as component carriers (CCs)) aggregately and simultaneously. An RF filter with multiple passbands, i.e., a multiband bandpass filter (MBPF), is a basic circuit that is expected to achieve broadband transmission such as CA using CCs in different frequency bands.

As a key device for supporting CA, the MBPF is required to have high performance such as sharp-skirt characteristics at the band-edges and a high degree of attenuation in the stopbands with low insertion losses in the passbands, which is remarkable when a wireless system with a high transmitter power is assigned to the frequency band between the two passbands of the MBPF. A high-temperature superconducting (HTS) filter is a

potential candidate that satisfies these requirements (Abu-Hudrouss, Jayyousi & Lancaster, 2008).

It is indispensable to investigate the nonlinear characteristics of the HTS filter because intermodulation distortion (IMD) is caused by the nonlinear characteristics of the HTS materials when applying the HTS filter to mobile communication systems. To measure the nonlinear characteristics, there are two common techniques (Wilker, Shen, Pang, Holstein & Face, 1995): one is the IMD measurement method using a signal with two tones and the other is the single tone harmonic generation measurement method. It is desirable to utilize the IMD measurement method using a signal with two closely-spaced tones in evaluating the nonlinear characteristics of the HTS filter since it might attenuate the power level of the harmonic components of the single tone.

The authors have shown the IMD characteristics of the 2.0-/3.5-GHz band HTS-DBPF with a YBCO thin film deposited on a MgO substrate when two signals are individually and simultaneously input to the center of the lower passband and the center of

higher passband as initial research on evaluating the IMD characteristics of an MBPF (Sato, Takagi, Narahashi & Nojima, 2011; Sato, Takagi & Narahashi, 2012a; Sato, Takagi, Narahashi & Nojima, 2012b).

This paper presents an experimental investigation on the IMD of the proposed 2.0-/3.5-GHz band HTS-DBPF. Measurement results show that the third-order IMD (IMD3) characteristics are generated differently depending on how the two-tone signal with a 30-kHz separation is input to the HTS-DBPF. The two ways that the signal is input to the HTS-DBPF are that the two-tone signals are individually input to either the 2.0-GHz band or 3.5-GHz band, or the two tone signals are simultaneously input to both the 2.0-GHz band and 3.5-GHz band. This paper also presents a method for estimating the IMD3 characteristics based on the third-order polynomial approximation of the input-output characteristics of the HTS-DBPF.

2 RESONATOR FOR HTS-DBPF

Figure 1 shows the resonator for the HTS-DBPF that has odd- and even-mode resonant frequencies (Sato et al., 2011). These two resonant modes have different current flows on the short stub.

This suggests that different current flows allow not only independent configuration of the coupling coefficients for the lower and higher passbands but also suppression of the IMD when a signal is simultaneously input to each passband.

3 IMD MEASUREMENTS

3.1 Measurement System

Figure 2 shows a block diagram of a two-tone IMD measurement system with a fundamental signal cancellation circuit for a single-band bandpass filter (Blount, Olson, Tshudy, Foote & Trantanella, 2004; Futatsumori, Furuno, Hikage, Nojima, Akasegawa, Nakanishi & Yamanaka, 2009). This measurement system enables measurement of the IMD characteristics without the nonlinear effect of the spectrum analyzer because two fundamental signals can be suppressed by more than 60 dB. By using the fundamental signal cancellation circuit, the IMD characteristics could be measured in detail at low power levels.

Figure 3 shows a new block diagram of two kinds of two-tone IMD measurement systems with a fundamental signal cancellation circuit for each

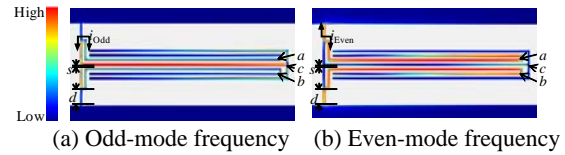


Figure 1: Resonator structure and current density distribution.

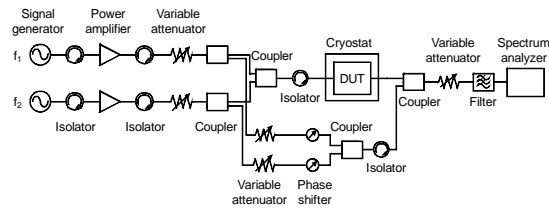


Figure 2: Block diagram for measuring IMD characteristics of single-band bandpass filter.

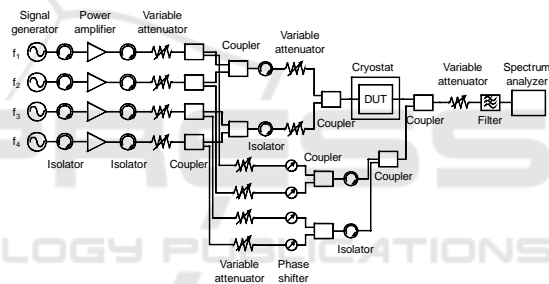


Figure 3: Block diagram for measuring IMD characteristics of dual-band bandpass filter.

passband in order to evaluate nonlinear characteristics when the two kinds of two-tone fundamental signals are input to each passband of the HTS-DBPF.

Figure 4 is a photograph of the configuration for the IMD measurement. This measurement system also enables measurement of the IMD characteristics with a wide dynamic range.

3.2 Measured Results

Figure 5 shows the measured IMD characteristics of the HTS-DBPF together with the ideal IMD3 characteristics. Here, the line with the slope of the third order fitted to the measured results at each passband represent the ideal IMD3 characteristics. In Figure 5(a), blue and red squares represent the third-order IMD (IMD3) characteristics for the 2.0-GHz band and 3.5-GHz band of the HTS-DBPF when a

two-tone fundamental signal with the separation of 30-kHz is input to the 2.0-GHz and 3.5-GHz passbands, respectively. The input and output power per tone are represented on the horizontal and



Figure 4: Experimental configuration for IMD measurement.

vertical axes, respectively. The measured IMD characteristics nearly coincide with the ideal distortion. The third-order input intercept point (IIP3) for the 3.5-GHz passband is +50 dBm at 60 K, while the IIP3 for the 2.0-GHz passband is +43 dBm. If the same IMD is assumed for each passband, the HTS-DBPF can handle an approximately 2.9-times higher input signal power in the 3.5-GHz passband than that in the 2.0-GHz passband at 60 K.

Figure 5(b) shows the measured IMD3 characteristics for both passbands of the HTS-DBPF when two kinds of two-tone fundamental signals (1957.795- and 1957.825-MHz signals for the 2.0-GHz passband, and 3463.515- and 3463.545-MHz signals for the 3.5-GHz passband) are simultaneously input to each passband. The total input power to the HTS-DBPF in Figure 5(b) is 3 dB higher than that in Figure 5(a). The IIP3 for the 3.5-GHz passband is higher than that for the 2.0-GHz passband. Based on Figure 5, the HTS-DBPF has almost the same IIP3 of approximately +43 dBm in the 2.0-GHz passband. If the same IMD is assumed for each passband, the power level of the input signal is defined by the IIP3 for the 2.0-GHz passband.

3.3 IMD3 Estimation

As shown in Figure 5, the IMD3 characteristics are generated differently depending on how the two-tone signal is input to the HTS-DBPF. This section

estimates the IMD3 characteristics shown in Figure 5(b) based on the polynomial approximation of the input-output characteristics of the HTS-DBPF.

If a two-tone signal with equal separation is input to each passband of an MBPF that has n passbands, the following two combinations represent

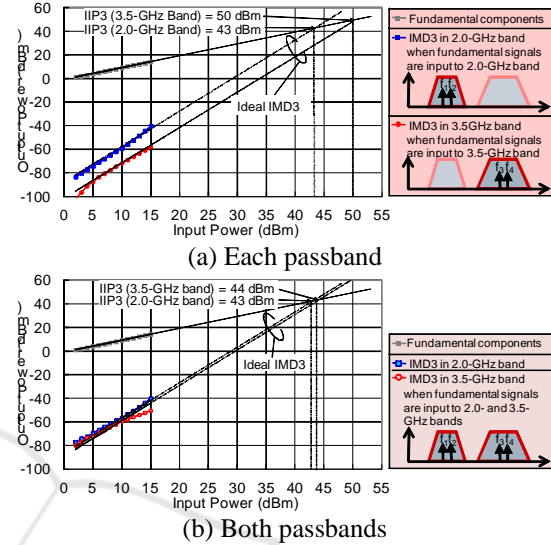


Figure 5: Measured IMD of HTS-DBPF using 30-kHz separated signals at 60 K.

the frequency components of the IMD3 characteristics generated in the vicinity of the two-tone signal at each passband.

$$\begin{aligned}
 & \text{(i)} \quad 2\omega_{i1} - \omega_{i2}, \quad 2\omega_{i2} - \omega_{i1} \\
 & \text{(ii)} \quad \omega_{i1} + \omega_{j1} - \omega_{j2}, \quad \omega_{i2} + \omega_{j2} - \omega_{j1} \quad (1) \\
 & \quad \quad \quad (i, j = 1, \dots, n, \quad i \neq j)
 \end{aligned}$$

where ω_{i1} and ω_{i2} ($\omega_{i1} < \omega_{i2}$) represent the angular frequencies of the first and second tones at the i -th passband, respectively. Here, the input signal, $x_i(t)$, to the i -th passband is assumed to be defined as

$$x_i(t) = a_{i1} \cos(\omega_{i1}t + \phi_{i1}) + a_{i2} \cos(\omega_{i2}t + \phi_{i2}) \quad (2)$$

where a_{i1} and a_{i2} , and ϕ_{i1} and ϕ_{i2} represent the amplitudes and phases of the two-tone signal, respectively. Assuming that the input-output characteristics of the HTS-MBPF can be expressed by the third-order polynomial approximation, the output signal, $y_i(t)$, of the i -th passband of the MBPF is given as

$$y_i(t) = b_{1i}x_i(t) + b_{3i}x_i^3(t) \quad (3)$$

where parameters b_{1i} and b_{3i} are defined as the coefficients of the first-order term and the third-order term of $x_i(t)$ derived from the measured IMD3 characteristics when $x_i(t)$ is input to the i -th passband, respectively. Then, the total output signal, $y(t)$, of the HTS-MBPF can be approximated as

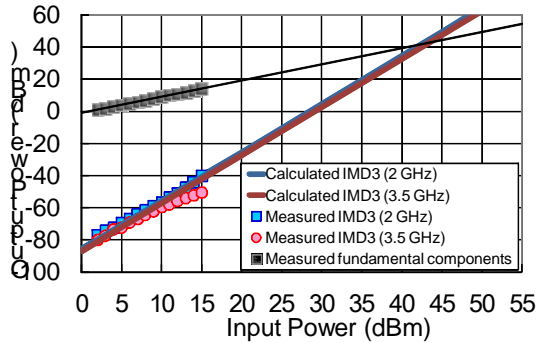


Figure 6: Measured and calculated IMD3 for 2-GHz band and 3.5-GHz band.

$$y(t) = \sum_{i=1}^n b_{1i} x_i(t) + \left(\sum_{i=1}^n b_{3i}^{1/3} x_i(t) \right)^3. \quad (4)$$

Figure 6 shows the measured and calculated IMD3 characteristics for each passband as well as the fundamental components of the HTS-DBPF using Equation (4) and parameters b_{1i} and b_{3i} ($i = 1, 2$). Comparing Figure 5(a) to Figure 5(b) leads to the fact that the IMD3 characteristics are almost the same in the 2-GHz band whereas they are 15.1 dB higher in the 3.5-GHz band at the input power level of 5 dBm. This difference is calculated as 16.6 dB using Eq. (4), which indicates good agreement between the measured and calculated results. The increase in the IMD3 characteristics in the 3.5-GHz band is considered to be due to the following reason. The IMD3 components generated by the combination of angular frequency $\omega_{21} + \omega_{11} - \omega_{12}$ (which depends on parameter b_{31}) appear at the angular frequency of $2\omega_{11} - \omega_{12}$ since parameter b_{31} is 4.9-times (13.7 dB) greater than parameter b_{32} .

4 CONCLUSIONS

This paper presented an experimental investigation on the IMD characteristics of an HTS-DBPF. A new two-tone IMD measurement system enables the evaluation of the IMD characteristics of the HTS-DBPF when the HTS-DBPF simultaneously deals

with two kinds of two-tone fundamental signals. This paper also presented a method for estimating the IMD3 characteristics based on the third-order polynomial approximation of the input-output characteristics of the HTS-DBPF.

There still remain technical issues such as clarifying the effective range of the HTS-DBPF using widely-separated signals or a modulated signal, investigating the nonlinearity of the HTS-DBPF when interference signals are input to its passband and when signals are input to its passband edges or stopbands, and confirming whether or not the proposed IMD3 estimation method is available when the two-tone signal employs a frequency separation other than 30 kHz.

REFERENCES

- Miki, N., Iwamura, M., Kishiyama, Y., Anil, U., and Ishii, H. 2010. *CA for Bandwidth Extension in LTE-Advanced*. NTT DOCOMO Technical Journal, 12(2), 10-19.
- Abu-Hudrouss, A. M., Jayyousi A. B., and Lancaster M. J. 2008. *Triple-Band HTS Filter Using Dual Spiral Resonators with Capacitive-Loading*. IEEE Trans. Appl. Supercond., 18(3), 1728-32.
- Wilker, C., Shen, Z., Pang, P., Holstein, W. L., and Face, D. W. 1995. *Nonlinear Effects in High Temperature Superconductors: 3rd Order Intercept from Harmonic Generation*. IEEE Trans. Appl. Supercond., 5(2), 1665-70.
- Satoh, K., Takagi, Y., Narahashi, S., and Nojima, T. 2011. *Intermodulation Distortion Characteristics of High-Temperature Superconducting Dual-Band Bandpass Filter*. Proc. of CJMW.
- Satoh, K., Takagi, Y., and Narahashi, S. 2012a. *Experimental Investigation of the Intermodulation Distortion Characteristics of High-Temperature Superconducting Dual-Band Bandpass Filter*. Proc. of TJMW, FR4-6.
- Satoh, K., Takagi, Y., Narahashi, S., and Nojima, T. 2012b. *Experimental Investigation of the Relationship between Operating Temperature and Power Handling Capability of High-Temperature Superconducting Dual-Band Bandpass Filter*. Physics Procedia, 36, 13-18.
- Blount, P., Olson, M., Tshudy, R., Foote, D., and Trantanella, C. 2004. *An Automated Phase Cancellation Method for Measuring Ultra-High Third Order Intercept Points*. IEEE MTT-S Int. Microwave Symp. Dig., 1727-30.
- Futatsumori, S., Furuno, M., Hikage, T., Nojima, T., Akasegawa, A., Nakanishi, T., and Yamanaka, K. 2009. *Precise Measurement of IMD Behavior in 5-GHz HTS Resonators and Evaluation of Nonlinear Microwave Characteristics*. IEEE Trans. Appl. Supercond., 19(3), 3595-99.